

Cracking of III-nitride layers with strain gradients

A. E. Romanov,^{a)} G. E. Beltz, P. Cantu,^{b)} F. Wu, S. Keller,
S. P. DenBaars, and J. S. Speck^{c)}

College of Engineering, University of California, Santa Barbara, California 93106

(Received 24 March 2006; accepted 20 July 2006; published online 20 October 2006)

Experimental results are demonstrated for the cracking of nominally compressed $\text{Al}_y\text{Ga}_{1-y}\text{N}$ layers grown on $\text{Al}_x\text{Ga}_{1-x}\text{N}$ buffer layers with smaller lattice constants ($y < x$). The authors present a theoretical analysis showing that the inclination of pure edge threading dislocation lines effectively reduces the compressive stress, causing relaxation, and after reaching a certain thickness begins to generate the tensile stress gradient responsible for cracking. The critical layer thickness for crack nucleation in such a gradient elastic field has been found. The results of the modeling are in good agreement with experimental observations of crack onset in nominally compressed nitride layers.

© 2006 American Institute of Physics. [DOI: 10.1063/1.2352043]

Nitride semiconductors, i.e., GaN and its ternary alloys, $\text{In}_x\text{Ga}_{1-x}\text{N}$ and $\text{Al}_y\text{Ga}_{1-y}\text{N}$, are now widely used for creating new generation of electronic and optoelectronic devices. Large differences in lattice parameters between different alloy compositions and between the nitride layer and substrate give rise to a high level of elastic strains and corresponding mechanical stresses. As the layer growth proceeds, the increase in stored elastic energy may initiate various relaxation processes in the layer or substrate.¹ For nitride semiconductors the observed relaxation phenomena include misfit dislocation (MD) formation at the layer interfaces^{2,3} or cracking in the layer.^{4,5} Both of these phenomena are not completely understood in the case of mismatched nitride layers. Typically, (0001) oriented III-nitride layers have a high density of threading dislocations (TDs), which are commonly a consequence of the coalescence of relaxed islands in the Volmer-Weber growth of the III-nitride directly on foreign substrates or on foreign substrates with nucleation layers.^{6,7}

The most intriguing problem in the cracking of nitride layers is that it occurs in layers under nominal compression (for a discussion of this issue refer to Ref. 8). In an early study, Itoh *et al.* argued that cracks initiated in the substrate, which was under tension.⁴ However, for thin layers tensile stresses in relatively thick substrates are negligibly small. Subsequent experiments^{5,8} confirmed that cracks nucleated at the surface of the growing films in the modes typical for fracture under tensile load (e.g., as shown in detail in Ref. 9). To explain these observations, Romano *et al.* proposed that the stress state changed in the nitride layers with increasing thickness.⁵ One possible mechanism of the development of tensile stresses in the growing layers was originally proposed by Hoffman as long as four decades ago.¹⁰ It addresses the elastic strains and stresses arising at the stage of island coalescence provided that the layer grows in island mode. However, as it will be shown below, cracking can be observed in nominally compressed $\text{Al}_y\text{Ga}_{1-y}\text{N}$ films, which are similar to those studied in Refs. 11–13 and which grew in a step-flow mode. It was demonstrated in our previous work^{12,14} that stress relaxation in nominally compressed layers can be

achieved via TD inclination, which leads to a gradual reduction of the compressive stress. Further layer growth with “frozen-in” inclined TDs will lead to the manifestation of a gradient in tensile stress, which at certain thickness can initiate layer cracking. The aims of the present letter are to report on the observation of cracking in nominally compressed layers with strain gradients and to develop a model for the critical thickness for the crack nucleation in such layers.

Si-doped $\text{Al}_{0.49}\text{Ga}_{0.51}\text{N}/\text{Al}_{0.62}\text{Ga}_{0.38}\text{N}$ layers were grown on *c*-plane sapphire substrates by low pressure metal organic chemical vapor deposition. Trimethylgallium (TMG) and trimethylaluminum (TMA) were used as the group III precursors, while ammonia (NH_3) was the group V precursor. Disilane ($\text{DiSi}=\text{Si}_2\text{H}_6$) was used for Si doping. The reactor pressure was kept constant at 100 Torr. The buffer layer growth was carried out in a H_2 ambient using a normal two-step process, where the deposition of a 16 nm thick AlGaN (Al content ~60%) nucleation layer at 600 °C was followed by an ~0.95 μm thick $\text{Al}_{0.62}\text{Ga}_{0.38}\text{N}$ buffer layer grown at 1150 °C with TMG and TMA flows of 28 and 60 μmol/min and no Si doping. Then a 136 nm thick $\text{Al}_{0.62}\text{Ga}_{0.38}\text{N}$ was grown with the same TMG and TMA flows and a DiSi flow of 5.5 μmol/min, resulting in a silicon concentration of $3 \times 10^{19} \text{ cm}^{-3}$ in the epitaxial layer as determined by secondary ion mass spectroscopy. Then, either 130 nm thick or 750 nm thick Si-doped $\text{Al}_{0.49}\text{Ga}_{0.51}\text{N}$ films were grown in a N_2 ambient on top of the buffer layer at 1150 °C, using a TMG flow of 10 μmol/min, a TMA flow of 12 μmol/min, and a DiSi flow of 6.7 μmol/min, corresponding to a silicon concentration of $1.2 \times 10^{20} \text{ cm}^{-3}$ in the film. The NH_3 flow was kept constant at 0.045 mol/min for all layers. All structural studies showed that these layers grew in a step-flow mode. The structural properties of the Si-doped $\text{Al}_{0.49}\text{Ga}_{0.51}\text{N}$ films were evaluated by atomic force microscopy, high-resolution x-ray diffraction, and transmission electron microscopy (TEM).

The relaxation in the $\text{Al}_{0.49}\text{Ga}_{0.51}\text{N}$ layer relative to the underlying $\text{Al}_{0.62}\text{Ga}_{0.38}\text{N}$ layer was determined by a combination of on-axis (0001) ω -2θ scans and reciprocal space maps in the vicinity of the (1015) reflection (see Refs. 11 and 12 for more details). The degree of relaxation R (where $R = 1$ corresponds to fully relaxed and $R = 0$ corresponds to

^{a)}Permanent address: Ioffe Physico-Technical Institute RAS, 194021 St. Petersburg, Russia.

^{b)}Present address: Cree Inc., 4600 Silicon Drive, Durham, NC 27703.

^{c)}Electronic mail: speck@mrl.ucsb.edu

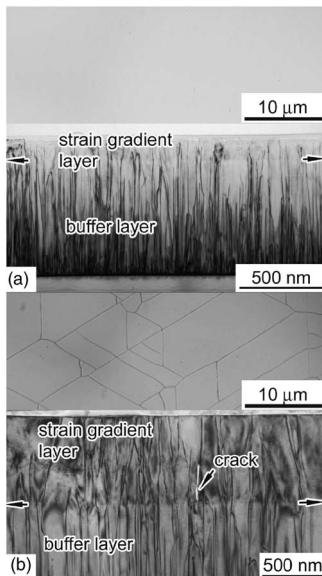


FIG. 1. Optical micrographs (top) and cross-section TEM images of $\text{Al}_{0.49}\text{Ga}_{0.51}\text{N}/\text{Al}_{0.62}\text{Ga}_{0.38}\text{N}$ layers recorded with $\mathbf{g}=(0002)$ two-beam imaging conditions. The thicknesses of the $\text{Al}_{0.49}\text{Ga}_{0.51}\text{N}$ layer are (a) ~ 130 nm and (b) ~ 750 nm. The 130 nm thick $\text{Al}_{0.49}\text{Ga}_{0.51}\text{N}$ layer did not show any cracking whereas the 750 nm thick $\text{Al}_{0.49}\text{Ga}_{0.51}\text{N}$ layer showed cracks which extended from mid-film thickness to the interface with the underlying $\text{Al}_{0.62}\text{Ga}_{0.38}\text{N}$ layer.

fully coherent) for both the 130 and 750 nm thick layers was $R=1.01$, indicating no elastic strain at the layer surface. For our zero order approximation, we have taken the main contribution in the formation of Bragg reflection coming from the near surface film region. Therefore we attribute R to this subsurface region of the film and compare this further with strain calculated exactly at the surface. In this simplified picture averaging over the layer thickness is excluded from the model. Optical microscopy studies of the 130 nm thick layer [Fig. 1(a)] showed no cracking whereas optical microscopy of the 750 nm thick layer showed cracks with an $\sim 20 \mu\text{m}$ spacing [Fig. 1(b)]. We attribute the similar relaxation for the 130 and 750 nm films to the cracking of the 750 nm thick film. Cracks in the film can relieve normal film stresses for lateral dimensions several times the film thickness. Cross-section TEM studies of the sample with the nominally 130 nm thick layer, Fig. 1(a), showed that the TDs inclined in the $\text{Al}_{0.49}\text{Ga}_{0.51}\text{N}$ layer. In contrast, the sample with the 750 nm thick layer, Fig. 1(b), also showed inclined TDs in the $\text{Al}_{0.49}\text{Ga}_{0.51}\text{N}$ layers but also showed cracks with openings from mid-depth in the $\text{Al}_{0.49}\text{Ga}_{0.51}\text{N}$ layer to the bottom of the $\text{Al}_{0.49}\text{Ga}_{0.51}\text{N}$ layer. The occluded crack indicated that the layer cracked during growth, providing stress relief, and then the crack was laterally overgrown.

An approach to understand stress relaxation via TD inclination in nominally compressed (0001) oriented nitride layers has been originally described in Ref. 11 and then developed in detail in Refs. 12 and 14. It was argued that stress relaxation occurs by the inclined segments of edge TDs with Burgers vectors of the type $(1/3)\langle 11\bar{2}0 \rangle$. In the buffer layer, these TDs have a [0001] line direction; however, in the compressed layer, they become systematically inclined with respect to the [0001] growth direction by some angle α . In plan view inclined TDs look like MD segments oriented along $\langle 1\bar{1}00 \rangle$ -type directions. The analysis given in Ref. 12 shows

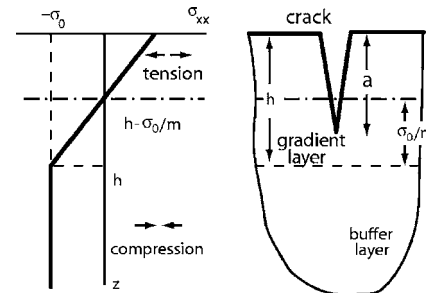


FIG. 2. Schematics showing (a) the stress gradient in a layer of thickness h and (b) cracking in the layer with the stress gradient.

that inclined TDs will be responsible for the relaxation plastic strain gradient:

$$\nabla \varepsilon_{\text{pl}} = \frac{1}{2} b \rho_{\text{TD}} \tan \alpha, \quad (1)$$

where b is the magnitude of TD Burgers vectors and ρ_{TD} is the TD density. As a result of the plastic relaxation, the elastic strain gradient leads to the following strain dependence on position inside the layer with inclined TDs:

$$\varepsilon_{xx} = \varepsilon_{yy} = \nabla \varepsilon_{\text{pl}}(h - z) - \varepsilon_m, \quad (2)$$

where h is the thickness of the layer with inclined TDs, ε_m is the magnitude of the initial compressive strain in the layer, e.g., due to the lattice mismatch with respect to the underlying buffer layer, and z is the coordinate counted from the layer surface (see Fig. 2). The gradient in strain relaxation $\nabla \varepsilon_{\text{pl}}$ can be determined from Eq. (1), but it also can be easily estimated from $\nabla \varepsilon_{\text{pl}} = \varepsilon_m/h_0$, where h_0 is the layer thickness of complete strain relaxation (zero elastic strain) on its surface. Stresses in the layer have similar behavior:

$$\sigma_{xx} = \sigma_{yy} = m(h - z) - \sigma_0, \quad z < h, \quad (3)$$

$$\sigma_{xx} = \sigma_{yy} = -\sigma_0, \quad z \geq h,$$

where we assume that linear stress dependence is in the layer of thickness h (see Fig. 2), m is stress gradient defined as $m = \sigma_0/h_0$, and σ_0 is the initial magnitude of compressive stresses that is related to equibiaxial mismatch ε_m :

$$\sigma_0 = \frac{(C_{11} + C_{12})C_{33} - 2C_{13}^2}{C_{33}} \varepsilon_m, \quad (4)$$

where C_{kl} are elastic constants for wurtzite-type semiconductors.

The value of σ_0 can be estimated, for example, for $\text{Al}_{0.49}\text{Ga}_{0.51}\text{N}$ layer, which is matched to $\text{Al}_{0.62}\text{Ga}_{0.38}\text{N}$ buffer. In this case $\varepsilon_m \approx 0.0032$ (Ref. 12) and C_{11} , C_{12} , C_{13} , and C_{33} for the layer ternary composition can be obtained by applying Vegard's law to the known constants for GaN and AlN (Ref. 15) that results in $\sigma_0 \approx 1.47 \text{ GPa}$. The stress gradient can be estimated by taking the experimentally determined¹² value of $h_0 \approx 130 \text{ nm}$ that gives $m \approx 11.3 \text{ GPa}/\mu\text{m}$ (or 10^{15} Pa/m). It is obvious that if the stress gradient is sustained during further layer growth, a high level of tensile stress can be generated in the subsurface part of the layer.

We now consider the case when the tensile stress on the surface is sufficient to induce cracking [as shown in Fig. 2(b)]. We limit our consideration to plane strain, wherein the crack front is relatively long along the y axis and the crack plane remains perpendicular to the x axis. We consider the

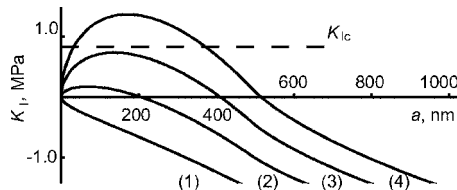


FIG. 3. Dependence of the stress intensity factor K_I on crack length a for an initial stress $\sigma_0=1.4$ GPa and stress gradient $m=7 \times 10^{15}$ Pa/m with varying layer thickness h : (1) 300 nm, (2) 400 nm, (3) 500 nm, and (4) 600 nm. The fracture toughness for GaN $K_{Ic}=0.8$ MPa $m^{1/2}$ (Ref. 18) is given by the dashed line.

“edging” mode as described in Ref. 9. The presence of a tensile stress field perpendicular to the crack plane implies that some mode I stress intensity factor K_I will be induced at the crack tip that would be indicative of a driving force for crack extension, in accordance with linear elastic fracture mechanics theory. The stress intensity would depend on several variables, such as layer thickness h , the magnitude of the internal compressive stress σ_0 , the stress gradient m and the crack length a . The stress intensity factor for a crack of prescribed length a can be determined through a superposition procedure outlined by Anderson,¹⁶ and is given by

$$K_I = \int_0^a \frac{2\sigma(\lambda)F(\lambda/a)}{\sqrt{\pi a}\sqrt{1-(\lambda/a)^2}} d\lambda, \quad (5)$$

where $\sigma(\lambda)=\sigma_{xx}$ is the stress along the plane in the *un-cracked* solid where the crack is envisaged to occur, as given by Eq. (3). Equation (5) is also rooted in the “weight” function theory developed in Ref. 17. The requisite weight function is given, for example, in Ref. 18, with $F(\xi) \approx 1.3 - 0.3\xi^{5/4}$. After some algebraic manipulation (e.g., see Ref. 19), Eq. (5) can be written in terms of a nonsingular integrand as

$$K_I = \sigma(a)\sqrt{\pi a} + \frac{2}{\sqrt{\pi a}} \int_0^a \frac{[\sigma(\lambda)F(\lambda/a) - \sigma(a)]}{\sqrt{1-(\lambda/a)^2}} d\lambda. \quad (6)$$

The integration can be performed analytically for gradient stress given by Eq. (3), this analytical solution will be presented elsewhere.

An example of the numerical results for $K_I(a)$ is shown in Fig. 3. As a general trend, K_I initially increases with crack size, i.e., the driving force increases as the crack grows. After reaching a maximum, the driving force decreases with increasing crack size. In all cases, it is expected that crack arrest would occur, if any growth occurs at all. One can define a critical thickness for cracking h_{crit} by identifying the maximum K_I with the critical stress intensity factor for fracture (or fracture toughness), K_{Ic} , and solving for h :

$$h_{\text{crit}} = \frac{\sigma_0}{m} + \frac{3\pi^{1/3}[2 + 0.6f_2(1)]^{1/3}}{[\pi + 0.6f_1(1)]} \left(\frac{K_{Ic}}{2m} \right)^{2/3}, \quad (7)$$

where the functions f_1 and f_2 are related to hypergeometric function ${}_2F_1$ and have numerical values $f_1(1) \approx 0.64$ and $f_2(1) \approx 0.25$. For layer thicknesses less than h_{crit} , the driving force for crack propagation remains insufficient to initiate fracture. Note that the first term of Eq. (7) is just h_0 , i.e.,

critical thickness may be given in the following form: $h_{\text{crit}} = h_0 + \Delta h_{\text{crit}}$.

Substituting the above mentioned value for stress gradient, $m \approx 11.3$ GPa/ μm , together with an experimentally found fracture toughness for GaN, $K_{Ic} \approx 0.8$ MPa $m^{1/2}$,²⁰ in Eq. (7) gives $\Delta h_{\text{crit}} \approx 173$ nm, i.e., $h_{\text{crit}} \approx 303$ nm. This result is consistent with our experimental observations, which show that nominally compressed $\text{Al}_{0.49}\text{Ga}_{0.51}\text{N}$ layers with inclined TDs remained crack-free for the thicknesses below ~ 300 nm, but demonstrated cracks for thicknesses on the order of 400 nm.

The proposed mechanism of crack nucleation in nominally compressed layers with strain gradients will operate only when TDs maintain in their frozen-in inclined orientation. The reason why TDs do not change their direction when the sign of the stress changes from compression to tension is unresolved. One speculation is that the growth with frozen-in TDs is governed by local processes in the vicinity of TD intersection with a layer surface. For a discussion we can comment that some data in the literature also indicated the presence of inclined TDs in initially compressed nitride layer, e.g., as those shown in Fig. 3(c) in Ref. 5 (but not noted by the authors in that time), undergoing tensile stress state with increasing the thickness.

The work was supported by the DARPA Suvos program (H. Temkin, program manager). Support for one of the authors (F.W.) was provided by the JST/ERATO program at UCSB. Another author (A.E.R.) was supported in part by RFBR Project No. 05-08-65503-a. The authors acknowledge the support of the National Science Foundation through the MRSEC Facilities.

¹A. E. Romanov, Z. Metallkd. **96**, 455 (2005).

²S. Srinivasan, L. Geng, R. Liu, F. A. Ponce, Y. Narukawa, and S. Tanaka, Appl. Phys. Lett. **83**, 5187 (2003).

³J. A. Floro, D. M. Follstaedt, P. Provencio, S. J. Hearne, and S. R. Lee, J. Appl. Phys. **96**, 7087 (2004).

⁴N. Itoh, J. C. Rhee, T. Kawabata, and S. Koike, J. Appl. Phys. **58**, 1828 (1985).

⁵L. T. Romano, C. G. Van de Walle, J. W. Ager III, W. Gotz, and R. S. Kern, J. Appl. Phys. **87**, 7745 (2000).

⁶X. H. Wu, P. Fini, E. J. Tarsa, B. Heying, S. Keller, U. K. Mishra, S. P. DenBaars, and J. S. Speck, J. Cryst. Growth **189/190**, 231 (1998).

⁷B. Moran, F. Wu, A. E. Romanov, U. K. Mishra, S. P. DenBaars, and J. S. Speck, J. Cryst. Growth **273**, 38 (2004).

⁸E. V. Etzorn and D. R. Clarke, J. Appl. Phys. **89**, 1025 (2001).

⁹J. W. Hutchinson and Z. Suo, Adv. Appl. Mech. **29**, 63 (1992).

¹⁰R. W. Hoffman, in *Physics of Thin Films*, edited by G. Haas and R. E. Thun (Academic, New York, 1966), Vol. 3, pp. 211–273.

¹¹P. Cantu, F. Wu, P. Walterteit, S. Keller, A. E. Romanov, U. K. Mishra, S. P. DenBaars, and J. S. Speck, Appl. Phys. Lett. **83**, 674 (2003).

¹²P. Cantu, F. Wu, P. Walterteit, S. Keller, A. E. Romanov, S. P. DenBaars, and J. S. Speck, J. Appl. Phys. **97**, 103534 (2005).

¹³D. M. Follstadt, S. R. Lee, P. P. Provencio, A. A. Allerman, J. A. Floro, and M. H. Crawford, Appl. Phys. Lett. **87**, 121112 (2005).

¹⁴A. E. Romanov and J. S. Speck, Appl. Phys. Lett. **83**, 2569 (2003).

¹⁵A. F. Wright, J. Appl. Phys. **82**, 2833 (1997).

¹⁶T. L. Anderson, *Fracture Mechanics: Fundamentals and Applications*, 2nd ed. (CRC, Ann Arbor, 1995).

¹⁷H. F. Bueckner, Z. Angew. Math. Mech. **50**, 529 (1970).

¹⁸H. Tada, P. C. Paris, and G. R. Irwin, *The Stress Analysis of Cracks Handbook*, 3rd ed. (ASME, New York, 2000).

¹⁹A. J. Monkowski and G. E. Beltz, Int. J. Solids Struct. **42**, 581 (2005).

²⁰M. D. Drory, J. W. Ager III, T. Suski, I. Grzegory, and S. Porowsky, Appl. Phys. Lett. **69**, 4044 (1996).